Larhyss Journal, ISSN 1112-3680, n°45, Mars 2021, pp. 141-163

DISCHARGE MEASUREMENT IN A RECTANGULAR OPEN-CHANNEL USING A SHARP-EDGED WIDTH CONSTRICTION THEORY AND EXPERIMENTAL VALIDATION

MESURE DU DEBIT DANS UN CANAL RECTANGULAIRE A L'AIDE D'UNE CONTRACTION DE LARGEUR A BORD VIF. THEORIE ET VALIDATION EXPERIMENTALE

ACHOUR B.[1], AMARA L.[2]

[1] Professor, Research laboratory in subterranean and surface hydraulics (LARHYSS), University of Biskra, Algeria.
[2] Associate Professor, Department of Civil Engineering and Hydraulics, Faculty of Science and Technology, University of Jijel, Algeria.

bachir.achour@larhyss.net

Research Article – Available at http://larhyss.net/ojs/index.php/larhyss/index
Received December 1, 2020, Received in revised form March 12, 2021, Accepted March 15, 2021

ABSTRACT

Flow measurement in open channels can be performed using a variety of devices such as multi-shaped weirs or hydraulic jump flow meters. Most of them have a sill at which solid deposits can accumulate. Self-Cleaning devices are those with a flat bottom which also corresponds to the bottom of the channel in which they are inserted. There is no bottom elevation in these devices. It is one of these devices that the present study sets out to examine from both a theoretical and an experimental point of view. It is a lateral contraction formed by a thin plate with a full central opening of width b placed perpendicular to the flow in a rectangular channel of width B. It is the simplest device that can be used for flow measurement. The theory is based on taking into account two sections, one located upstream of the device and the other taken to the right of the opening where critical flow could take place. The head loss caused between these two sections is not negligible, but current knowledge does not allow it to be evaluated. For this reason, this head loss is neglected in the theoretical development. By writing the equality of the heads between the two previously mentioned sections and introducing the dimensionless parameter h_1^*, a third degree equation in h_1^* is obtained. This equation is written in the following functional form $\psi(h_1^*, B/b) = 0$. The dimensionless parameter h_1^* represents the ratio between the depth h_1 and the critical depth h_c in the initial section. Thus, for a given value of the contraction rate B / b, h_1^* is a constant. This fact is corroborated by experimental tests. The only real root to consider from the third degree equation is such that $h_1^* > 1$ because the flow is subcritical in the initial section upstream of the device. In addition, the theoretical development clearly shows that the discharge coefficient C_d of the device is closely related to h_1^* by an explicit relation. In other words, knowing the value of the ratio *B/b*, h_1^* is then given by solving the third degree equation, and consequently the discharge coefficient C_d is then worked out.

The theoretical development is confronted with the results of the tests carried out on eight devices whose contraction rate *b / B* varies between 0.15 and 0.45. The main conclusion to retain is that the maximum relative deviation between theoretical and experimental discharge coefficients is less than 2%. All the observed relative deviations are taken into account in the fitting of the theoretical discharge coefficient relationship.

Keywords: Flow measurement, discharge, flow meter, discharge coefficient, sharp edge, width constriction.

RESUME

La mesure du débit dans les canaux ouverts peut être effectuée à l'aide de divers dispositifs tels que des déversoirs à formes multiples ou des débitmètres à sauts hydrauliques. La plupart d'entre eux ont un seuil sur lequel les dépôts solides peuvent s'accumuler. Les dispositifs autonettoyants sont ceux à fond plat qui correspond également au fond du canal dans lequel ils sont insérés. Il n'y a pas d'élévation de fond dans ces appareils. C'est l'un de ces dispositifs que la présente étude se propose d'examiner à la fois d'un point de vue théorique et expérimental. Il s'agit d'une contraction latérale formée par une plaque mince avec une ouverture centrale pleine de largeur b placée perpendiculairement à l'écoulement dans un canal rectangulaire de largeur B. C'est le dispositif le plus simple qui puisse être utilisé pour la mesure du débit. La théorie repose sur la prise en compte de deux sections, l'une située en amont de l'appareil et l'autre prise au droit de l'ouverture où un écoulement critique pourrait avoir lieu. La perte de charge induite entre ces deux sections n'est pas négligeable, mais les connaissances actuelles ne permettent pas de l'évaluer. Pour cette raison, cette perte de charge est négligée par le développement théorique. En écrivant l'égalité des charges entre les deux sections précédemment mentionnées et en introduisant le paramètre sans dimension h_1^*, une équation du troisième degré est obtenue. Cette équation est écrite sous la forme fonctionnelle suivante $\psi(h_1^*, B/b) = 0$. Le paramètre sans dimension h_1^* représente le rapport entre la profondeur h_1 et la profondeur critique h_c dans la section initiale. Ainsi, pour une valeur donnée du taux de contraction *B/b*, h_1^* est une constante. Ce fait est corroboré par des tests expérimentaux. La seule racine réelle à considérer à partir de l'équation du troisième degré est telle que $h_1^* > 1$ car l'écoulement est fluvial dans la section initiale en amont de l'appareil. De plus, le développement théorique montre clairement que le coefficient de débit C_d du dispositif est étroitement lié à h_1^* par une relation explicite. En d'autres termes, connaissant la valeur du rapport *B/b*, h_1^* est alors donnée en résolvant l'équation du troisième degré, et par conséquent le coefficient de débit C_d est alors déduit.

Le développement théorique est confronté aux résultats des tests effectués sur huit appareils dont le taux de contraction *b/B* varie entre 0,15 et 0,45. La principale conclusion à retenir est que l'écart relatif maximal entre les coefficients de débit théoriques et expérimentaux est inférieur à 2%. Tous les écarts relatifs observés sont pris en compte dans l'ajustement de la relation du coefficient de débit théorique.

Mots clés : Mesure de débit, débit, débitmètre, coefficient de débit, arête vive, rétrécissement de largeur.

INTRODUCTION

In free-surface hydraulics, measuring the flow rate through a channel is a common problem encountered in the practice of the hydraulic engineer. Knowledge of the flow rate is required for determining the discharge capacity of a given channel or for establishing the synthetic curve of the head-discharge law of the channel.

In the case of a uniform flow, it is accepted that the flow rate through a given channel depends on five parameters which are: the depth of the flow, the geometric slope of the channel, the absolute roughness of the walls of the channel, the linear dimensions of the channel and finally the viscosity of the flowing liquid. From these five parameters, the flow calculation is then possible by using one of the usual formulas for uniform flow.

However, in practice, several devices can be used to estimate the flow rate through a given channel and which is the same as that which passes through the device used. Among the wide variety of devices available today, it is possible to find the one which would best meet the requirements imposed by the user and capable in particular of providing the required precision in the measurement of the desired flow rate. The most used devices are either constituted by a thin plate of rectangular notched shape, or by a broad-crested sill, the most common shape of which is either rectangular or triangular (Bouslah, 2006; Achour et al., 2003; Kechida, 2006; Achour 2013). Their placement through a flow causes a raise of the upstream level of water, the free discharge of which downstream is obtained by means of thin-walled devices. The best known of these is certainly the sharp-crested V-notched weir known as Thomson weir (Bos, 1976; 1989; De Coursey and Blanchard, 1970; Rao, 1963), the precision of which is sufficient for both low and high heads.

A thin plate with lateral constriction is also one of the simple devices designed to measure the flow rate in open channels, particularly rectangular channels due to the easier implementation (Vallentine, 1958; Hachemi Rachedi, 2006). These studies are purely experimental and aimed to define the Depth-discharge law of the device. The first study seems unreliable for several reasons, such as the low flow rates which were varied between 0.708 l/s and 2.24 l/s and the shallow depths tested, the average of which is only 10 cm. Extrapolation of the results derived from this study to practical cases where flow rates can reach an average of 30 l/s to 40 l/s does not seem possible. The results of this study should be viewed with great caution. On the other hand, the second study is more reliable because the tested flow rates and depths are in the practical range. The experimental results of this study will be used herein in order to validate the theoretical development.

In practice, it is also used the so-called hydraulic jump flow meters to measure the flow rate in open channels. With the exception of Achour's hydraulic jump flow meter (Achour, 1989) whose cross section shape is triangular, hydraulic jump flow meters are often of rectangular shape. The best known of these are the Venturi and Parshall (Bos, 1976) or the modified Venturi (Hager, 1985). These devices have the ability to not only measure the flow rate but also to raise the level of the downstream flow which is a real advantage in low slope areas (Achour, 1989).

In general, the use of the above-mentioned devices is to measure the depth of the flow in an upstream section after their placement in the considered channel. By measuring this upstream flow depth and knowing the geometric characteristics of the device, it is then possible to estimate the flow rate by applying the Depth-Discharge relationship. For these reasons, the devices are called semi-modular as opposed to modular devices whose flow rate depends only on their geometric characteristics.

In this study, a thin lateral constriction plate used as measuring discharge device in a rectangular open channel is theoretically examined. The theoretical development aims to establish both the discharge and the discharge coefficient relationships. A theoretical development is proposed which will be supported by an experimental validation based on the tests of Hachemi-Rachedi (2006).

DESCRIPTION OF THE DEVICE AND THE FLOW

Fig. 1 shows a perspective view of the studied device. This is inserted in a cross section of a rectangular channel of width B and of which it is desired to evaluate the flow rate.

The device consists of two thin-walled projections placed on either side of the walls of the channel. A rectangular notch of width b appears between the two projections of the device. This notch has a flat floor, i.e. without any bottom elevation, unlike conventional flow measurement devices. The placement of the measuring device in the canal causes a reduction or a narrowing of its cross-section. The ratio $b/B = \beta$ defines the rate of contraction of the section of the canal at the site of the installation of the device. The rate of contraction can also be defined as $\sigma = 1 - b/B = 1- \beta$. When the opening width is 0, i.e. $b = 0$, corresponding to $\beta = 0$, the contraction rate is $\sigma = 1$, indicating that the entire section of the canal is entirely closed. On the other hand, when the width of the notch is equal to B ($b = B$), corresponding to $\beta = 1$, the contraction rate is $\sigma = 0$, indicating that all the section of the channel is entirely open. It is therefore possible to note that the dimensionless parameter β is such that $0 \leq \beta \leq 1$ or that the parameter σ is such that $0 \leq \sigma \leq 1$.

One can also note that thanks to the geometry of the device under consideration, the longitudinal axis of the channel is not affected and remains horizontal over the entire length of the channel, from upstream to downstream and through the notch of the device. This particularity is interesting because it avoids any solid deposit which could be entrained by the flow. This geometry therefore gives the device a self-Cleaning character.

In order to observe in more detail the flow upstream, downstream and at the location of the device, we present on photographs (1) to (3) some views of this flow. Photograph 1 clearly shows the subcritical nature of the flow in the measurement channel, immediately upstream of the device. This state of flow can be observed for all devices tested. It also shows the supercritical nature of the flow downstream of the device as well as the mass of water surrounding the liquid layer crossing it. This body of water can be observed in the photograph 2. The mass of water surrounding the overflow is created because the liquid streams of the poured water fall on those of the bottom flow. The contraction is incomplete since the liquid streams of the bottom flow are directly drawn towards the outlet of notch, without undergoing contraction in the central axis of the notch. When falling, the liquid streams of the headwater interfere with the natural development of the bottom streamlines which have no other possibilities than to expand laterally by occupying the free space located on either side of the overflow water body. The liquid mass can take non-negligible proportions, depending on the value of the pouring head as well as that of the contraction rate β.

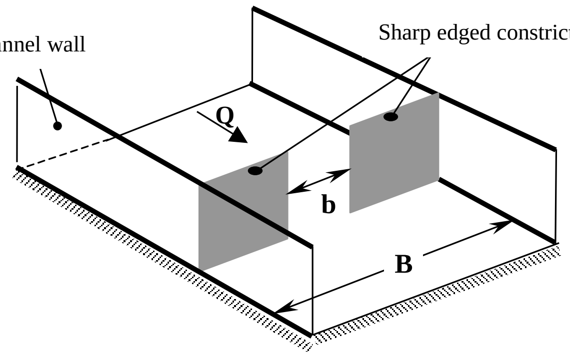

Figure 1: Definition sketch of a sharp edged constriction in a rectangular channel

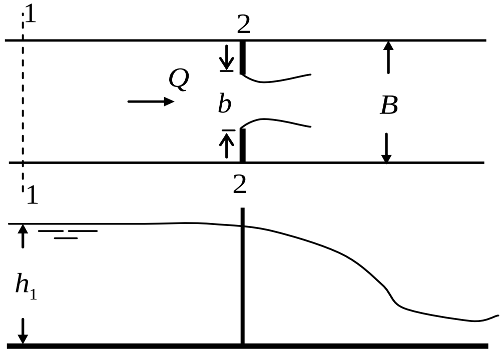

Figure 2: Plan view of the channel and the device as well as the longitudinal profile of the flow

Photo 1: Plan view of the device placed in a rectangular supply channel. View of the forced contraction of the flow.

Photo 2: View of the flow upstream and downstream of the device. Flow from right to left.

Photo 3: Side view of the contracted flow crossing the notch of the device

THEORETICAL DEPTH-DISCHARGE RELATIONSHIP

The critical depth in the rectangular cross-section 1-1 (Fig. 2) is written as:

$$h_{1c} = \left(\frac{Q^2}{g B^2} \right)^{1/3} \tag{1}$$

Where the subscript « *c* » denotes the critical conditions.

On the other hand, the critical depth in the rectangular cross-section 2-2 is as:

$$h_{2c} = \left(\frac{Q^2}{g b^2} \right)^{1/3} \tag{2}$$

The ratio of relations (1) and (2) gives:

$$\frac{h_{1c}}{h_{2c}} = (b / B)^{2/3} \tag{3}$$

Resulting in:

$$h_{2c} = h_{1c} (B / b)^{2/3} \tag{4}$$

Assume that there is no pressure drop between sections 1-1 and 2-2. Equal total heads between sections 1-1 and 2-2 translates into:

$$H_1 = H_2 = \frac{3}{2} h_{2c} \tag{5}$$

Combining Eqs. (4) and (5) results in:

$$H_1 = \frac{3}{2} h_{1c} (B / b)^{2/3} \tag{6}$$

Hence:

$$\frac{H_1}{h_{1c}} = \frac{3}{2} (B / b)^{2/3} \tag{7}$$

The total head H_1 can be written as:

$$H_1 = h_1 + \frac{Q^2}{2 g B^2 h_1^2} \tag{8}$$

Implying that:

$$\frac{H_1}{h_{1c}} = \frac{h_1}{h_{1c}} + \frac{Q^2}{2 g B^2 h_1^2 h_{1c}} \tag{9}$$

Eq. (1) allows writing that:

$$\frac{Q^2}{gB^2} = h_{1c}^3 \tag{10}$$

Combining Eqs. (9) and (10) yields:

$$\frac{H_1}{h_{1c}} = \frac{h_1}{h_{1c}} + \frac{1}{2(h_1 / h_{1c})^2} \tag{11}$$

Eqs. (7) and (11) give what follows:

$$\frac{H_1}{h_{1c}} = \frac{h_1}{h_{1c}} + \frac{1}{2(h_1 / h_{1c})^2} = \frac{3}{2}(B / b)^{2/3} \tag{12}$$

Let us adopt the following non-dimensional parameter

$$h_1 / h_{1c} = h_1^* \tag{13}$$

Inserting Eq. (13) into Eq. (12) results in:

$$h_1^* + \frac{1}{2h_1^{*2}} = \frac{3}{2}(B / b)^{2/3} \tag{14}$$

Eq. (14) shows that the non-dimensional parameter h_1^* only depends on the ratio B/b. Note that the flow in the section 1-1 is subcritical, meaning that $h_1 > h_{1c}$ or $h_1^* > 1$.

Eq. (14) is represented graphically in figure 3. It shows that the non-dimensional parameter h_1^* increases with the increase of the ratio B / b .

Figure 3: Variation of $h_1^*(B / b)$ according to Eq. (14)

Eq. (14) can be rewritten as:

$$h_1^{*3}-\frac{3}{2}(B/b)^{2/3}h_1^{*2}+\frac{1}{2}=0 \tag{15}$$

It is a third order equation of the form:

$$z^3+az^2+bz+c=0 \tag{16}$$

Where: $a=-\frac{3}{2}(B/b)^{2/3}$; $b=0$; $c=1/2$

To find the solutions of equation (15), use the method described by Spiegel (1974). Let us assume the following parameters:

$$H=\frac{3b-a^2}{9}=-\frac{9(B/b)^{4/3}}{4\times 9}=-\frac{(B/b)^{4/3}}{4} \tag{17}$$

$$R=\frac{9ab-27c-2a^3}{54}=\frac{-27c-2a^3}{54}=\frac{-27/2+2(27/8)(B/b)^2}{54}$$

Thus:

$$R=\frac{1}{8}\left[(B/b)^2-2\right] \tag{18}$$

Let's find the angle α such that:

$$\cos\alpha=+\frac{R}{\sqrt{-H^3}}=\frac{\frac{1}{8}\left[(B/b)^2-2\right]}{\sqrt{\frac{(B/b)^4}{64}}}=-\frac{\left[(B/b)^2-2\right]}{(B/b)^2}=1-2(B/b)^{-2} \tag{19}$$

That is:

$$\alpha=\cos^{-1}\left[1-2(B/b)^{-2}\right] \tag{20}$$

The discriminant of equation (16) is expressed as:

$$\Delta=H^3+R^2 \tag{21}$$

Inserting Eqs. (17) and (18) into Eq. (21) and rearranging, one may obtain:

$$\Delta=\frac{1}{16}\left[1-(B/b)^2\right]=\frac{1}{16}(1-B/b)(1+B/b) \tag{22}$$

Eq. (22) shows that the discriminant Δ is equal to zero in the case where $B/b = 1$. But, this is a trivial case which does not interest our study. The study is focussed on cases where the ratio B / b is greater than 1, which means that Δ is negative according to Eq. (22). In this case, Eq. (16) has three real roots which are given as:

$$z_1 = 2\sqrt{-H}\cos(\alpha/3) - a/3 \tag{23}$$

$$z_2 = 2\sqrt{-H}\cos(\alpha/3 + 240°) - a/3 \tag{24}$$

$$z_3 = 2\sqrt{-H}\cos(\alpha/3 + 120°) - a/3 \tag{25}$$

Whence:

$$z_1 = \left(B/b\right)^{2/3}\left[\cos\left(\frac{1}{3}\cos^{-1}\left[1-2(B/b)^{-2}\right]\right)+\frac{1}{2}\right] = h^*_{1;1} \tag{26}$$

$$z_2 = \left(B/b\right)^{2/3}\left[\cos\left(\frac{1}{3}\cos^{-1}\left[1-2(B/b)^{-2}\right]+240°\right)+\frac{1}{2}\right] = h^*_{1;2} \tag{27}$$

$$z_3 = \left(B/b\right)^{2/3}\left[\cos\left(\frac{1}{3}\cos^{-1}\left[1-2(B/b)^{-2}\right]+120°\right)+\frac{1}{2}\right] = h^*_{1;3} \tag{28}$$

For a given configuration indicated in Figure 2, there is obviously only one solution to choose among the three solutions given by equations (26), (27), and (28). It is the one that corresponds to $h_1^* > 1$.

Eq. (1) allows writing that:

$$Q = \sqrt{g}Bh_{1c}^{3/2} \tag{29}$$

Taking into account Eq. (13), Eq. (29) becomes:

$$Q = \sqrt{g}B\frac{h_1^{3/2}}{h_1^{*3/2}} \tag{30}$$

Eq. (30) can be rewritten as:

$$Q = C_d\sqrt{2g}Bh_1^{3/2} \tag{31}$$

Eq. (31) is the theoretical depth-discharge relationship for the studied device, where C_d is the discharge coefficient expressed as:

$$C_d = \frac{1}{\sqrt{2}\,h_1^{*3/2}} \tag{32}$$

The upstream depth h_1 of the flow is measured by a simple point gauge reading at the inlet of the device.

As the dimensionless parameter h_1^* is governed by Eqs. (26), (27), and (28), on may conclude that the discharge coefficient C_d depends only on the *B/b* ratio. Eqs. (26), (27), and (28), along with Eq. (32), allow computing the discharge coefficient C_d some values of which are given in table 1.

Table 1: Some theoretical values of the discharge coefficient C_d

h_1^*	***B/b***	C_d
1	1	0.70710678
1.1	1.01325224	0.61290897
1.2	1.04759195	0.53791435
1.3	1.09737351	0.47705667
1.4	1.15904493	0.42686736
1.5	1.23025997	0.38490018
1.6	1.30940258	0.34938562
1.7	1.39531861	0.31901538
1.8	1.48715746	0.29280349
1.9	1.5842748	0.2699943
1.905	1.58925976	0.26893203
1.91	1.59425659	0.26787671
2	1.6861706	0.25

Figure 4 shows the graphical representation of the $C_d(B/b)$ theoretical relationship.

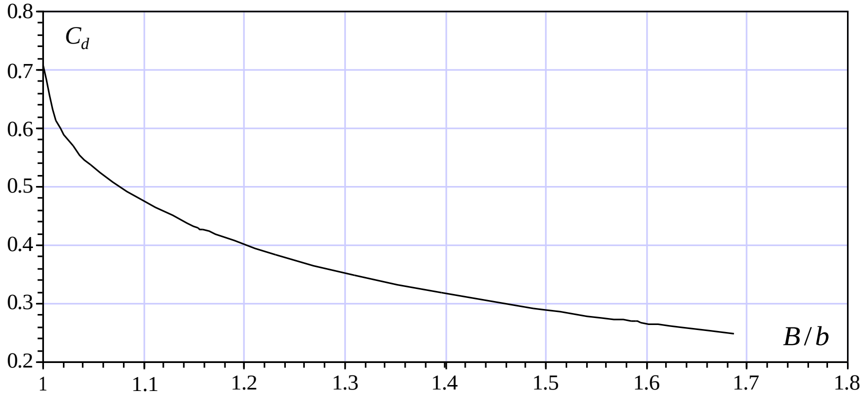

Figure 4: Variation of the discharge coefficient $C_d(B/b)$ for the studied device

Fig. 4 shows that the discharge coefficient C_d decreases with the increase of the *B/b* ratio, which is consistent with the physical meaning. For a given channel, the increase in the *B / b* ratio is due to the decrease in the output width *b* of the device. The decrease in *b* causes a slowing down of the upstream flow, which has the consequence of reducing the discharge coefficient C_d .

EXPERIMENTAL VALIDATION

The experimental validation of the theoretical development is based on the highly significant tests of Hachemi-Rachedi (2006). In a rectangular channel of width *B* = 29.3 cm, depth 48.5 cm and length of 12 m, eight devices were tested the characteristics of which are as follows:

Table 2: Geometric characteristics of the tested devices

***b* (cm)**	4.40	5.30	5.90	7.40	8.80	10.25	11.70	13.20
$\beta = b/B$	0.150	0.181	0.201	0.253	0.300	0.350	0.400	0.450

The upstream depths h_1 were measured using a double-precision Vernier gauge, graduated to 1/10th. The geometry of the devices tested had the particularity of making the body of water upstream of the device almost horizontal, eliminating any disturbance of the free surface. This undoubtedly contributed to a better precision in the reading of the depths by means of the gauge used.

The flow rates were measured using an ultrasonic flowmeter whose precision varies between 0.1 l/s and 0.2 l/s. The flow rates were varied between 1.6 l/s and 28.20 l/s, while the depths h_1 were in the range 4.3 cm ≤ h_1 ≤ 33.02 cm. A sample of 157 pairs of (Q, h_1) values carried out during this experimentation.

The tests showed that for each tested contraction rate β, the dimensionless parameter h_1^* varied slightly around an average value whatever the flow rate, suggesting that h_1^* is a constant for a given value of β, as predicted by the present theory.

Table 3 groups together the values of the theoretical and experimental discharge coefficients C_d . Theoretical values of h_1^* were calculated using Eqs. (26) to (28), while theoretical discharge coefficient was worked out from Eq. (32). The experimental discharge coefficients were calculated by applying Eq. (31). For each device tested, a series of flow rates are obtained. Whatever the flow rate, Eq. (31) showed that the experimental discharge coefficient varying around an average value indicated in the table 3.

Table 3: Theoretical and experimental discharge coefficients values of the eight tested devices

b/B	*B/b*	h_1^* Theoretical	$C_{d,Th}$ Theoretical	$C_{d,Exp}$ Experimental	$\Delta C_d / C_d$ %
0.15017065	6.65909091	5.29141031	0.05809354	0.0570793	1.745874373
0.18088737	5.52830189	4.66683175	0.07013774	0.0695507	0.836985804
0.20136519	4.96610169	4.33963042	0.07821785	0.07712	1.403582367
0.25255973	3.95945946	3.71805925	0.09863034	0.0970981	1.553520799
0.3003413	3.32954545	3.2986833	0.11802502	0.1172322	0.671735921
0.34982935	2.85853659	2.96435539	0.1385446	0.13678	1.273668291
0.39931741	2.5042735	2.69745485	0.15960766	0.1580833	0.955066142
0.45051195	2.21969697	2.47062157	0.18208562	0.1784486	1.997425276

Table 3 shows that the theoretical discharge coefficients $C_{d,Th}$ are very slightly higher than the experimental discharge coefficients $C_{d,Exp}$. This is probably due to the head loss neglected during the theoretical development. The maximum relative deviation observed is of the order of 2% only.

The values of the theoretical and experimental discharge coefficients of table 3 are represented graphically in Fig. 5.

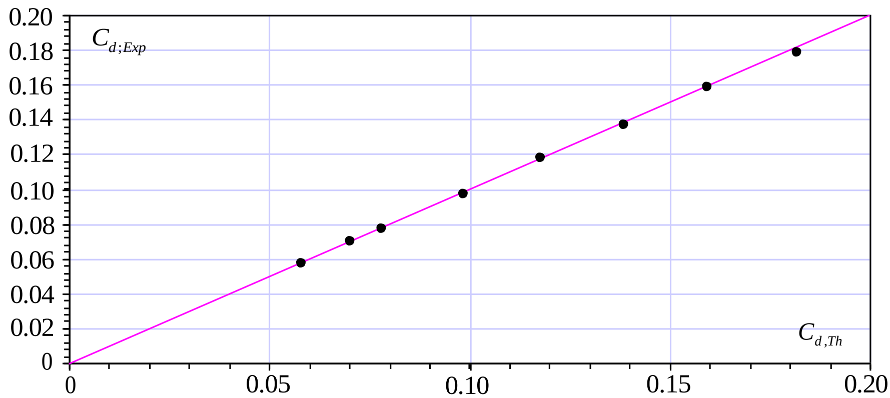

Figure 5: Variation of $C_{d,Exp}$ with $C_{d,Th}$ according to Table 3

Fig. 5 shows that the points $C_{d,Exp}$ and $C_{d,Th}$ are practically aligned on the first bisector (Red line) of equation $C_{d,Exp} = C_{d,Th}$. The points in figure 4 are governed satisfactorily by the following equation, with $R^2 = 0.9998$:

$$C_{d,Exp} = 0.9864 C_{d,Th} \tag{33}$$

Inserting Eq. (33) into Eq. (32) results in;

$$C_d = \frac{0.9864}{\sqrt{2}\, h_1^{*3/2}} = \frac{0.6975}{h_1^{*3/2}} = \varphi(B/b) \tag{34}$$

This is the final relationship of the discharge coefficient of the studied device. For a given value of *B/b*, one of the equations (26) to (28) gives the appropriate value of h_1^*. Thus, Eq. (34) allows calculating the discharge coefficient C_d of the considered device. Knowing the value of the discharge coefficient C_d, the measured upstream depth h_1, and the channel width *B*, Eq. (31) gives the required flow rate *Q*.

On the other hand, Eq. (31) can be rewritten as:

$$Q = C_d\left(\frac{B}{b}\right)\sqrt{2g}\, b h_1^{3/2} \tag{31a}$$

That is:

$$Q = \mu\sqrt{2g}\, b h_1^{3/2} \tag{31b}$$

Where:

$$\mu = C_d\left(\frac{B}{b}\right) \tag{35}$$

Combining Eqs. (34) and (35) results in:

$$\mu = \frac{0.6975(B/b)}{h_1^{*3/2}} = \psi(B/b) \tag{36}$$

NOTE

As shown in Table 3, the experimentation has more particularly interested in the low values of the parameter β such that $\beta = b/B < 1/2$. In fact, low values of β lead to large values of the upstream depth of the flow, which are therefore easy to measure. If in a rectangular channel the flow to be measured is associated with a shallow depth, the reading of the latter risks causing relatively large relative errors. In order to reduce these errors, it is recommended to raise the water level by installing a device with a small notch b and therefore a low value of β. In addition, the great depths linked to the low values of β induce a low value of the approaching flow velocity that can therefore be neglected without causing a significant error.

Vallentine (1958) indicates that no effect of the h_1/B ratio was observed on the discharge coefficient C_d. Hachem-Rachedi's tests (2006) have indeed corroborated this finding. There is no effect of either B/h_1 or b/h_1 ratio (Table 4). Note, however, that the authors Arun Goel and Verma (2015) claim having observed the influence of b/h_1 ratio on the discharge coefficient C_d. during tests carried out on a single device characterized by a contraction rate $\beta = b/B = 1/2$.

Table 4 gives some experimental characteristics of the flow for the case of the contraction rate $\beta = 0.15$. One observes in particular the clear variation of the ratio b/h_1 whereas the experimental discharge coefficient $C_{d,Exp}$. remains practically constant around the average value 0.0570793. This table confirms that the b/h_1 ratio has no effect on the discharge coefficient. This is the case for all the tested devices with a contraction rate such as $0.15 \leq \beta \leq 0.45$.

Table 4: Some experimental parameters for B = 29.3 cm, b = 4.4 cm, β = 0.15 (Hachemi-Rachedi, 2006)

Q (l/s)	h_1 (cm)	b / h_1	$C_{d,Exp}$
2.38333	9.938	0.44274502	0.0586164
3.21667	12.538	0.35093316	0.05582729
3.63333	13.218	0.33287941	0.05825584
4.2	14.858	0.29613676	0.05650562
4.48333	15.698	0.28029048	0.05554148
5.51667	17.674	0.24895326	0.05720808
5.96667	18.498	0.23786355	0.05778665
6.46667	19.598	0.22451271	0.05743091
7.03333	21.046	0.20906586	0.05612931
7.66667	22.132	0.19880716	0.05673597
8.4	23.598	0.18645648	0.0564611
9.03333	24.528	0.17938682	0.05729777
9.66667	25.782	0.1706617	0.05689639
10.58333	27.27	0.16134947	0.05726347
10.7	27.488	0.16006985	0.05720737
11.36667	28.574	0.15398614	0.05734023
12.13333	30.038	0.14648112	0.05678799
13.03333	31.162	0.14119761	0.05772985
13.18333	31.49	0.1397269	0.05748428

EXAMPLE 1

Determine the discharge coefficient C_d of the device represented by Figure 1, characterized by the widths ratio $B/b=\sqrt{2}$.

SOLUTION

Applying relations (26), (27), and (28) results respectively in:

$$h_{1;1}^{*}=\left(B/b\right)^{2/3}\left[\cos\left(\frac{1}{3}\cos^{-1}\left[1-2(B/b)^{-2}\right]\right)+\frac{1}{2}\right]$$

$$=\left(\sqrt{2}\right)^{2/3}\times\left[\cos\left(\frac{1}{3}\cos^{-1}\left[1-2\times(\sqrt{2})^{-2}\right]\right)+\frac{1}{2}\right]=1.72108416\approx 1.721$$

$$h_{1;2}^{*}=\left(B/b\right)^{2/3}\left[\cos\left(\frac{1}{3}\cos^{-1}\left[1-2(B/b)^{-2}\right]+240°\right)+\frac{1}{2}\right]$$

$$=\left(\sqrt{2}\right)^{2/3}\times\left[\cos\left(\frac{1}{3}\cos^{-1}\left[1-2\times(\sqrt{2})^{-2}\right]+240°\right)+\frac{1}{2}\right]=0.62996053\approx 0.630$$

$$h_{1;3}^{*}=\left(B/b\right)^{2/3}\left[\cos\left(\frac{1}{3}\cos^{-1}\left[1-2(B/b)^{-2}\right]+120°\right)+\frac{1}{2}\right]$$

$$h_{1;3}^{*}=\left(\sqrt{2}\right)^{2/3}\times\left[\cos\left(\frac{1}{3}\cos^{-1}\left[1-2\times(\sqrt{2})^{-2}\right]+120°\right)+\frac{1}{2}\right]=-0.46116311\approx -0.461$$

As mentioned before, h_1^* must be greater than 1. It is therefore the first solution that must be retained, namely:

$$h_1^*=1.72108416\approx 1.721$$

According to Eq. (34), the discharge coefficient C_d is as:

$$C_d=\frac{0.6975}{h_1^{*3/2}}=\frac{0.6975}{1.72108416^{3/2}}=0.30891646\approx 0.309$$

PHYSICAL MEANING OF THE DIMENSIONLESS PARAMETER h_1^*

To give the physical meaning of the dimensionless parameter h_1^*, let us recall for this the relation which governs the Froude number. This is written in section 1-1 of the device input as:

$$F_1^2 = \frac{Q^2}{gB^2 h_1^3} \tag{37}$$

Inserting Eq. (1) into Eq. (37) results in:

$$F_1^2 = \frac{h_{1c}^3}{h_1^3} = \frac{1}{(h_1 / h_{1c})^3} \tag{38}$$

Taking into account Eq. (13), Eq. (38) becomes:

$$F_1^2 = \frac{h_{1c}^3}{h_1^3} = h_1^{*-3} \tag{39}$$

Thus:

$$h_1^* = F_1^{-2/3} \tag{39a}$$

It is thus demonstrated that the dimensionless parameter h_1^* is closely related to the Froude number of the incident flow in the device.

Inserting Eq. (39a) into the fundamental relationship (15), yields:

$$F_1^{-2} - \frac{3}{2}(B/b)^{2/3} F_1^{-4/3} + \frac{1}{2} = 0 \tag{40}$$

After some rearrangements, Eq. (40) is reduced to:

$$F_1^2 - 3(B/b)^{2/3} F_1^{2/3} + 2 = 0 \tag{40a}$$

This is the relationship between the Froude number of the incident flow to the widths ratio B/b.

Let us assume the following change in variables:

$$X = F_1^{2/3} \tag{41}$$

Combining Eqs. (40a) and (41) results in:

$$X^3 - 3(B/b)^{2/3} X + 2 = 0 \quad (42)$$

One thus obtains a third degree equation in *X*, without second order, which can be solved according to the method described above. Taking into account the change in variables expressed by equation (41), one will obtain the relation of the Froude number of the incident flow as a function of the widths ratio B/b. As the flow at the entrance of the device is in subcritical regime, the incident Froude number F_1 must be less than 1.

Eq. (42) is in the following form:

$$X^3 + aX^2 + bX + c = 0 \quad (42a)$$

Where: $a = 0$; $b = -3(B/b)^{2/3}$, and $c = 2$.

Let us assume the following parameters:

$$H = \frac{3b - a^2}{9} = -\frac{3 \times 3(B/b)^{2/3}}{9} = -(B/b)^{2/3} \quad (43)$$

$$R = \frac{9ab - 27c - 2a^3}{54} = \frac{-27c}{54} = \frac{-27 \times 2}{54} = -1 \quad (44)$$

Let's find the angle α such that:

$$\cos\alpha = +\frac{R}{\sqrt{-H^3}} = -\frac{1}{\sqrt{(B/b)^2}} = -\left(B/b\right)^{-1} \quad (45)$$

That is:

$$\alpha = \cos^{-1}\left[-\left(B/b\right)^{-1}\right] \quad (45a)$$

The discriminant of equation (42a) is expressed as:

$$\Delta = H^3 + R^2 \quad (46)$$

Inserting Eqs. (40) and (41) into Eq. (21) and rearranging, one may obtain:

$$\Delta = \left[1 - \left(B/b\right)^2\right] = \left(1 - B/b\right)\left(1 + B/b\right) \quad (46a)$$

Eq. (46a) shows that the discriminant Δ is equal to zero in the case where $B/b = 1$. The study is focussed on cases where the ratio B/b is greater than 1, which means that Δ is negative according to Eq. (46a). In this case, Eq. (38) has three real roots which are given as:

$$X_1 = 2\sqrt{-H}\cos(\alpha/3) - a/3 \tag{47}$$

$$X_2 = 2\sqrt{-H}\cos(\alpha/3 + 240°) - a/3 \tag{48}$$

$$X_3 = 2\sqrt{-H}\cos(\alpha/3 + 120°) - a/3 \tag{49}$$

Whence:

$$X_1 = 2\left(B/b\right)^{1/3}\left[\cos\left(\frac{1}{3}\cos^{-1}\left[-(B/b)^{-1}\right]\right)\right] \tag{47a}$$

$$X_2 = 2\left(B/b\right)^{1/3}\left[\cos\left(\frac{1}{3}\cos^{-1}\left[-(B/b)^{-1}\right] + 240°\right)\right] \tag{48a}$$

$$X_3 = 2\left(B/b\right)^{1/3}\left[\cos\left(\frac{1}{3}\cos^{-1}\left[-(B/b)^{-1}\right] + 120°\right)\right] \tag{49a}$$

Taking into account the change in variables expresses by Eq. (41), the three solutions in F_1 are:

$$F_{1;1} = \left\{2\left(B/b\right)^{1/3}\cos\left(\frac{1}{3}\cos^{-1}\left[-(B/b)^{-1}\right]\right)\right\}^{3/2} \tag{50}$$

$$F_{1:2} = \left\{2\left(B/b\right)^{1/3}\cos\left(\frac{1}{3}\cos^{-1}\left[-(B/b)^{-1}\right] + 240°\right)\right\}^{3/2} \tag{51}$$

$$F_{1;3} = \left\{2\left(B/b\right)^{1/3}\cos\left(\frac{1}{3}\cos^{-1}\left[-(B/b)^{-1}\right] + 120°\right)\right\}^{3/2} \tag{52}$$

EXAMPLE 2

Compute the incident Froude number F_1 of the flow in the device inlet section 1-1 indicated in Figure 1 for the widths ratio $B/b = \sqrt{2}$.

SOLUTION

Applying Eqs. (50), (51), and (52) results respectively in:

$$F_{1;1} = \left\{2\left(B/b\right)^{1/3}\cos\left(\frac{1}{3}\cos^{-1}\left[-(B/b)^{-1}\right]\right)\right\}^{3/2}$$

Whence:

$$F_{1;1} = \left\{ 2 \times \left(\sqrt{2}\right)^{1/3} \times \cos\left(\frac{1}{3} \cos^{-1}\left[-(\sqrt{2})^{-1} \right] \right) \right\}^{3/2} = 2$$

$$F_{1:2} = \left\{ 2\left(B/b\right)^{1/3} \cos\left(\frac{1}{3} \cos^{-1}\left[-(B/b)^{-1} \right] + 240° \right) \right\}^{3/2}$$

Hence:

$$F_{1:2} = \left\{ 2 \times \left(\sqrt{2}\right)^{1/3} \times \cos\left(\frac{1}{3} \cos^{-1}\left[-(\sqrt{2})^{-1} \right] + 240° \right) \right\}^{3/2} = 0.44289098 \approx 0.443$$

$$F_{1;3} = \left\{ 2\left(B/b\right)^{1/3} \cos\left(\frac{1}{3} \cos^{-1}\left[-(B/b)^{-1} \right] + 120° \right) \right\}^{3/2}$$

Thus:

$$F_{1;3} = \left\{ 2 \times \left(\sqrt{2}\right)^{1/3} \times \cos\left(\frac{1}{3} \times \cos^{-1}\left[-(\sqrt{2})^{-1} \right] + 120° \right) \right\}^{3/2} = (-2.16843016)^{3/2}$$

The first equation gives $F_1 = 2$ which does not correspond to the subcritical character of the flow in the inlet section of the device. The third solution is mathematically and physically impossible. The obtained value of X is negative, which does not conform to the physical meaning of the relation (41) where F_1 must be positive. The second solution gives $F_1 < 1$, which corresponds to the physical reality since the flow at the entrance of the device, i.e. section 1-1 in Figure1, is subcritical. Therefore, the solution to the problem is given by the second equation, i.e. $F_1 = 0.443$.

Note that when combining Eqs. (34) and (39a) one may write:

$$C_d = 0.6975 F_1 \tag{53}$$

Therefore, the discharge coefficient C_d varies linearly as a function of the incident Froude number F_1. Considering the current case, Eq. (53) gives:

$$C_d = 0.6975 F_1 = 0.6975 \times 0.44289098 = 0.30891646 \approx 0.309$$

This is obviously the same value computed in example 1.

CONCLUSIONS

The study looked at a device for measuring the flow rate in a rectangular channel of width *B*. It is composed of a vertical thin plate with a central opening of width *b*, arranged perpendicular to the flow. The plate can be metallic, plastic or even concrete of the same type as that of the channel in which it is inserted. The device is therefore very simple to produce and to use. It is one of the simplest devices for measuring flow in an open rectangular channel.

The study has rigorously shown that both the flow rate and the discharge coefficient of such a device can be drawn from a theoretical development. The result shows that the device is semi-modular since the flow rate depends both on its geometric characteristics, i.e. the widths ratio *B/b*, and on the upstream flow depth. Characterized by a flat floor, the device is therefore self-cleaning.

Based on experimental tests given by the literature, it has been observed that the theoretical and experimental discharge coefficients deviate by only 2% at most. The theoretical discharge coefficient relationship has therefore been adjusted to be in accordance with the experimental observations.

It is to be noted that the study concerned contraction rate $\beta = b/B$ such as $0.15 \leq \beta \leq 0.45$. The authors of the present study do not claim that the theoretical relationships derived herein are strictly applicable and extrapolated for contraction rates $\beta \geq 1/2$. The theoretical development must therefore be subjected to an intense experimental program involving devices characterized by such contraction rates. The influence of the b/h_1 ratio could possibly be observed as mentioned by some authors for $\beta = 1/2$.

REFERENCES

ACHOUR B. (2013). Semi-modular rectangular broad-crested flow meter with lateral contraction, International Journal of Engineering and Technology Sciences, Vol. 1, Issue 5, pp. 310-323.

ACHOUR B. Débitmètre à ressaut en canal de section droite triangulaire sans seuil, Journal of Hydraulic Research (In French), Vol. 27, Issue 2, pp. 205-214.

ACHOUR B., BOUZIANE M.T., NEBBAR K. (2003). Broad-crested triangular flowmeter in rectangular channel, Larhyss Journal, No 3, pp. 7-43.

BAZIN H. (1898). Expériences nouvelles sur l'écoulement en déversoir, Edition Dunod, Paris, France.

BOS M.G. (1976). Discharge measurement structures, Laboratorium voor hydraulica aan Afvoerhydrologie, Landbouwhogeschool, Wageningen, The Netherlands, Report 4, May.

BOS M.G. (1989). Discharge measurement structure, 3rd Ed., Publication 20, Int. Institute for Land Reclamation and Improvement, Wageningen, Netherlands.

BOUSLAH S. (2006). Theoretical and experimental analysis of broad-crested triangular weir, Master Thesis, Department of hydraulics, University of Biskra, Algeria.

DE COURSEY D.E., BLANCHARD B.J. (1970). Flow analysis over large triangular weir, Proceedings ASCE, Journal of Hydraulic Division, Vol. 96, (HY7), pp. 1435-1454.

GOEL, D.V.S., SANJEEV SANGWAN V. (2015). Open Channel Flow Measurement of Water by Using Width Contraction, International Scholarly and Scientific Research & Innovation, World Academy of Science, Engineering and Technology, Vol. 9, Issue 2, pp. 1557-1562.

HACHEMI RACHEDI L. (2006). Flow analysis trough a lateral contraction, Master Thesis, Department of Hydraulics, University of Biskra, Algeria.

HAGER W.H. (1985). Modified Venturi channel, Proceedings ASCE, Journal of Irrigation and Drainage Engineering, Vol. 111, IR1, pp.19-35.

KECHIDA S. (2006). Theoretical and experimental analysis of a flow over a wide rectangular sill, Master Thesis, Department of Hydraulics, University of Biskra, Algeria.

KINDSVATER C.E., CARTER R.W. (1957). Discharge characteristics of rectangular thin-plate weirs, Proceedings ASCE, Journal of. Hydraulic Division, Vol. 83, (HY6), pp. 1453/1-6.

SIA. (1926). Contribution à l'étude des méthodes de jaugeage, Bulletin 18, Schw. Bureau Wasserforschung, Bernn, Switzerland.

RAO N.S.L. (1963). Theory of weir, Advances in hydrodynamics, Edition Ven Te Chow, New York, USA.

SPIEGEL M.R. (1974). Mathematical Handbook of Formulas and Tables, 20th Edition, McGraw Hill Inc, New York, USA.

VALLENTINE H.R. (1958). Flow in Rectangular Channels with Lateral Constriction Plates, La Houille Blanche, No 1, pp. 75-84.